Development/Plasticity/Repair

Lin28B and Let-7 in the Control of Sympathetic Neurogenesis and Neuroblastoma Development

Melanie Hennchen,[1] Jutta Stubbusch,[1,2,3] Ikram Abarchan-El Makhfi,[1] Marco Kramer,[1,2,3] Thomas Deller,[2] Cécile Pierre-Eugene,[5] Isabelle Janoueix-Lerosey,[5] Olivier Delattre,[5] Uwe Ernsberger,[1,2,3] Johannes B. Schulte,[4] and Hermann Rohrer[1,2,3]

[1]Developmental Neurobiology, Max Planck Institute for Brain Research, 60438 Frankfurt am Main, Germany, [2]Institute of Clinical Neuroanatomy, Goethe University of Frankfurt, 60590 Frankfurt am Main, Germany, [3]Ernst Strüngmann Institute, 60528 Frankfurt am Main, Germany, [4]Department of Pediatric Oncology and Haematology, Children's Hospital Essen, 45122 Essen, Germany, and [5]Unité Institut National de la Santé et de la Recherche Médicale, U830, Centre de Recherche Institut Curie, 75248 Paris Cedex 05, France

The RNA binding protein Lin28B is expressed in developing tissues and sustains stem and progenitor cell identity as a negative regulator of the *Let-7* family of microRNAs, which induces differentiation. Lin28B is activated in neuroblastoma (NB), a childhood tumor in sympathetic ganglia and adrenal medulla. Forced expression of Lin28B in embryonic mouse sympathoadrenal neuroblasts elicits postnatal NB formation. However, the normal function of Lin28B in the development of sympathetic neurons and chromaffin cells and the mechanisms involved in Lin28B-induced tumor formation are unclear. Here, we demonstrate a mirror-image expression of *Lin28B* and *Let-7a* in developing chick sympathetic ganglia. *Lin28B* expression is not restricted to undifferentiated progenitor cells but, is observed in proliferating noradrenergic neuroblasts. *Lin28* knockdown in cultured sympathetic neuroblasts decreases proliferation, whereas *Let-7* inhibition increases the proportion of neuroblasts in the cell cycle. Lin28B overexpression enhances proliferation, but only during a short developmental period, and it does not reduce *Let-7a*. Effects of *in vivo Lin28B* overexpression were analyzed in the *LSL-Lin28B*^{DBHiCre} mouse line. Sympathetic ganglion and adrenal medulla volume and the expression level of *Let-7a* were not altered, although *Lin28B* expression increased by 12- to 17-fold. In contrast, *Let-7a* expression was strongly reduced in *LSL-Lin28B*^{DbhiCre} NB tumor tissue. These data demonstrate essential functions for endogenous *Lin28* and *Let-7* in neuroblast proliferation. However, *Lin28B* overexpression neither sustains neuroblast proliferation nor affects let-7 expression. Thus, in contrast to other pediatric tumors, *Lin28B*-induced NB is not due to expansion of proliferating embryonic neuroblasts, and Let-7-independent functions are implicated during initial NB development.

Key words: **Let-7; Lin28; neuroblastoma; neurogenesis; proliferation; sympathetic**

Significance Statement

Lin28A/B proteins are highly expressed in early development and maintain progenitor cells by blocking the biogenesis and differentiation function of Let-7 microRNAs. Lin28B is aberrantly upregulated in the childhood tumor neuroblastoma (NB). NB develops in sympathetic ganglia and adrenal medulla and is elicited by forced Lin28B expression. We demonstrate that Lin28A/B and Let-7 are essential for sympathetic neuroblast proliferation during normal development. Unexpectedly, Lin28B upregulation in a mouse model does not affect neuroblast proliferation, ganglion size, and Let-7 expression during early postnatal development. Lin28B-induced NB, in contrast to other pediatric cancers, does not evolve from neuroblasts that continue to divide and involves Let-7-independent functions during initial development.

Introduction

Neuroblastoma (NB) is a childhood cancer that arises from cells of the developing sympathetic nervous system, and primary tumors are located in sympathetic ganglia and adrenal glands. NB presents a broad clinical spectrum, but aggressive metastatic tumors (S4)represent the majority of NB cases in older children, are still largely incurable, and account for about 10% of pediatric cancer-related deaths (Maris et al., 2007).

Received July 6, 2015; revised Nov. 4, 2015; accepted Nov. 10, 2015.

Author contributions: M.H., J.S., U.E., and H.R. designed research; M.H., J.S., I.A.-E.M., M.K., and C.P.-E. performed research; I.J.-L., O.D., and J.B.S. contributed unpublished reagents/analytic tools; M.H., J.S., I.A.-E.M., M.K., T.D., and H.R. analyzed data; M.H., J.S., T.D., I.J.-L., U.E., and H.R. wrote the paper.

This work was supported by grants from the Wilhelm Sander Foundation to H.R. We thank Melanie Bickel and Sabine Stanzel for excellent technical assistance and Julia Holzmann for comments on this manuscript.

Previous studies provided evidence for a role of the *Lin28B* gene in NB development. Genomic variations [small nucleotide polymorphisms (SNPs)] in the *Lin28B* gene influence susceptibility to NB development, and *Lin28B* expression levels are elevated in aggressive forms of NB and correlate with poor prognosis (Diskin et al., 2012). Association of *Lin28B* with advanced disease and poor clinical outcome has been demonstrated also for other tumor types, including pediatric cancers (Viswanathan et al., 2009; Zhou et al., 2013; Urbach et al., 2014). *Lin28B* emerged as an oncogenic driver for NB since forced expression of *Lin28B* in sympathoadrenal cells is sufficient to induce tumors with the gene expression pattern (*Dbh*, *Th*, *Phox2a*, *MYCN*) characteristic for NB in postnatal sympathetic ganglia and adrenals (Molenaar et al., 2012). Because the normal function of Lin28B during sympathetic nervous system development is not known, it remains unclear why sympathoadrenal cells are susceptible to genomic variations in the *Lin28B* gene and how *Lin28B* overexpression causes NB.

The RNA-binding proteins Lin28B and Lin28A (collectively called Lin28) are expressed in stem and progenitor cells and have essential functions in the maintenance of stem cell identity (Thornton and Gregory, 2012). The Lin28 proteins inhibit the biogenesis of *Let-7* family microRNAs, thereby interfering with progenitor differentiation and promoting stem cell growth. Conversely, Lin28 expression is antagonized by *Let-7*. This inverse regulatory relationship is well documented for stem cells in developing and tumor tissues (Viswanathan et al., 2009; Thornton and Gregory, 2012), but is also important for the timing of neuron production during nervous system development (La Torre et al., 2013). *Let-7* expression increases during neuron differentiation, and *Let-7* overexpression interferes with proliferation and elicits differentiation of neural stem cells in the mouse brain (Wulczyn et al., 2007; Rybak et al., 2008; Schwamborn et al., 2009; Zhao et al., 2010; La Torre et al., 2013). *Lin28* and *Let-7*, discovered in *Caenorhabditis elegans* as heterochronic genes that control cell fate succession, may thus have similar functions in the developing vertebrate nervous system (Balzer et al., 2010; La Torre et al., 2013). Although *Let-7*-suppression accounts for many Lin28 effects, Lin28 also binds and influences the translation of a large number of messenger RNAs, and *Let-7*-independent functions for Lin28B were described previously during brain and tumor development (Hafner et al., 2013; Nguyen et al., 2014; Yang et al., 2015).

In contrast to other lineages in the central and peripheral nervous system, neuron differentiation in sympathetic ganglia is not linked to cell cycle withdrawal (Rohrer, 2011). Neurogenesis proceeds mainly by proliferation of immature but already differentiated noradrenergic neuroblasts (Rothman et al., 1978; Rohrer and Thoenen, 1987). Undifferentiated progenitor cells are present only at the onset of neurogenesis (Tsarovina et al., 2008; Gonsalvez et al., 2013). Lin28B overexpression in embryonic sympathoadrenal cells elicits tumor formation in sympathetic ganglia and adrenal medulla (Molenaar et al., 2012). It was unclear, however, whether the timing and differentiation of sympathetic neuron development are controlled by endogenous Lin28 and *Let-7* and whether forced Lin28B expression leads to tumor initiation by interfering with terminal differentiation, as observed for other types of pediatric tumors (Viswanathan et al., 2009; Gillis et al., 2011; Urbach et al., 2014).

Here, we demonstrate essential functions for endogenous Lin28A/B and *Let-7* in sympathetic neuroblast proliferation. However, *Let-7a* expression is not affected *in vitro* and *in vivo* by *Lin28B* overexpression, and postnatal ganglia and adrenal medulla show normal size and differentiation in the *LSL-Lin28B*^{DbhiCre} mouse. Thus, in contrast to other pediatric cancers, Lin28B-induced NB development is not caused by a failure to differentiate and leave the cell cycle.

Materials and Methods

Transfection and culture of sympathetic ganglion cells. Sympathetic ganglia (SGs) from embryonic day 6.5 (E6.5) to E12 chicken embryos were dissected and dissociated by the use of 0.1% (w/v) trypsin as described previously (Rohrer and Thoenen, 1987; Zackenfels et al., 1995). Single cell suspensions were electroporated with the Amaxa Basic Neuron Small Cell Number (SCN) Nucleofector Kit (Program SCN 4). The following concentrations of DNA or RNA were used: pCAGGSggLin28B (0.5 μg/300,000 cells), pmaxGFP Vector (0.25 μg/300,000 cells), and empty pCAGGS vector (0.5 μg/300,000 cells) as control; miRCURYLNA Power family inhibitor hsa-let7 (10 pmol/200,000 cells; Exiqon) and, as control, miRCURYLNA inhibitor negative control B (30 pmol/200,000 cells; Exiqon); iBONI siRNA Quattro siggLin28A or B (50 pmol from each siRNA/300,000 cells; Riboxx) and, as control, iBONI siRNA Negative Control-N1 (200 pmol/300,000 cells; Riboxx); sensor mRNA Let7a and miR-1 (10 pmol/200,000 cells). After density step-gradient centrifugation to remove cell debris, 15,000 cells per well were plated on four-well culture dishes coated with 0.5 mg/ml poly-DL-ornithine (Sigma) in 0.15 M borate buffer, pH 8.3, and 10 μg/ml laminin (Invitrogen) in PBS, pH 7.3, and cultured in MEM, 1% (w/v) penicillin/streptomycin, 1% (w/v) glutamine, 10% (v/v) horse serum, and 5% (v/v) fetal calf serum (SG medium) for 2 d. Proliferating cells were detected by 5-ethinyl-2′-desoxyuridine (EdU) labeling using the Click-iT EdU Alexa Fluor 488 or 594 imaging kit (Invitrogen) as described previously (Reiff et al., 2011; Holzmann et al., 2015). The proportion of EdU-labeled neurons was quantified in at least three independent experiments and statistically analyzed using two-tailed Student's *t* test.

Detection of Let-7 *and* miR-1 *expression by RNA sensor.* To generate *Let-7* and *miR-1* sensor mRNA for transfection, a pSLU plasmid was used (kind gift from A. La Torre and T. Reh, University of Washington, Seattle, WA). To synthesize the sensor mRNA we used mMESSAGE mMACHINE T7 Ultra Kit from Ambion according to the manufacturer's instructions. To detect GFP, expressed by the *Let-7* or *mir-1* sensor mRNA, an immunostaining for GFP was performed. Cells were fixed with 4% (w/v) paraformaldehyde for 15 min, permeabilized with 0.25% (w/v) Triton X-100 (AppliChem) in PBS, washed twice with PBS, and blocked with 5% (v/v) goat serum in PBS for at least 1 h. The primary antibody against GFP (rb IgG polyclonal; Invitrogen; 1:400 in PBS) was incubated at RT for 1 h. After washing twice with PBS, the cells were incubated with Alexa 594-labeled secondary antibody (1:500; Invitrogen). Nuclei were stained by DAPI (Sanofi). The number of GFP-negative cells was quantified using a Zeiss Axiophot2 microscope in combination with a Visitron systems spot RT3 camera. Experiments were repeated independently at least three times and statistically analyzed using unpaired two-tailed Student's *t* test.

In situ *hybridization.* Chick embryos were staged according to Hamburger and Hamilton (1951) and fixed in 4% (w/v) paraformaldehyde in 0.1 M sodium phosphate buffer, pH 7.3, for 3 h or overnight, depending on the Hamburger-Hamilton (HH) stage. Embryos were subsequently dehydrated in 15% (w/v) sucrose in 0.1 M sodium phosphate buffer, pH 7.3. Whole embryos were embedded in Tissue Tec (Sakura Fintek), and cryosections of 12 μm from the brachial region were prepared for *in situ* hybridization. Riboprobes were synthesized from linearized plasmids by the use of a DIG RNA Labeling Kit (Roche) according to manufacturer's instructions. The following cRNA probes were used: *SCG10* (890 bp; *ggSCG10* kindly provided by A. Groves, Caltech, Pasadena, CA), *ggNotch1* (4 kb; Wakamatsu et al., 2000), *ggLin28A* (738 bp, correspond-

The authors declare no competing financial interests.

Correspondence should be addressed to Hermann Rohrer, Institute of Clinical Neuroanatomy, Goethe University Frankfurt/M, Theodor-Stern-Kai 7, 60590 Frankfurt am Main, Germany. E-mail: hermann.rohrer@brain.mpg.de.

DOI:10.1523/JNEUROSCI.2560-15.2015

 0270-6474/15/3516532-14$15.00/0

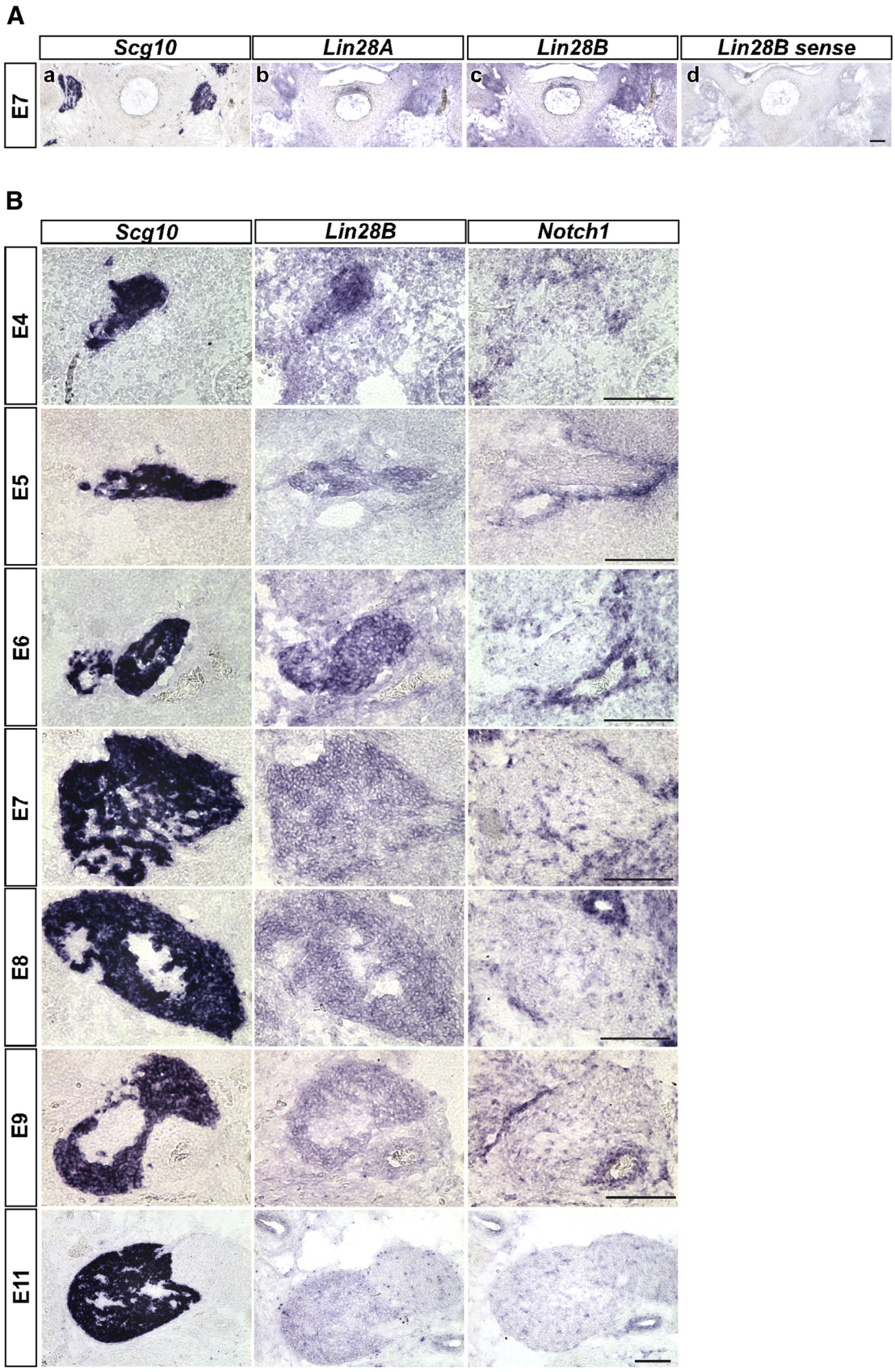

Figure 1. *Lin28B* expression in developing chick sympathetic ganglia. ***A***, *Lin28A* and *Lin28B* are coexpressed in sympathetic ganglia at E7. Parallel sections were stained for the neuronal marker *SCG10* to identify the ganglion location. ***B***, The expression of *Lin28B* was analyzed by *in situ* hybridization on frozen sections of E4–E11 chick embryos. *SCG10* was used to identify the ganglion location. *Notch1* was used as marker for sympathetic progenitors. *Lin28B* is broadly expressed throughout the ganglia. The *Lin28B* hybridization signal decreases between E7 and E11. Scale bars, 100 μm.

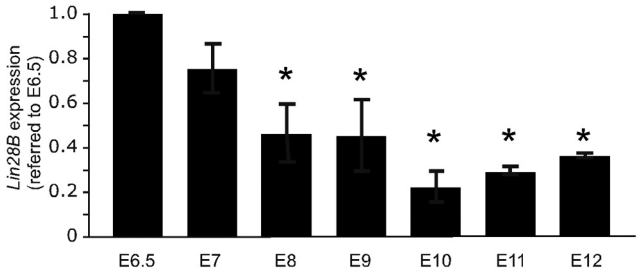

Figure 2. Analysis of *Lin28B* expression in developing chick sympathetic ganglia by qRT-PCR. *Lin28B* mRNA expression was quantified by RT-qPCR at E6.5, E7, E8, E9, E10, E11, and E12 and normalized to *Gapdh*. *Lin28B* expression levels were significantly reduced from E8 onward compared to E6.5 levels (mean ± SEM; $n = 3$; statistical analysis by relative expression software REST). $*p < 0.05$.

ing to base 444–1182 of NM_001031774), and *ggLin28*B (711 bp, corresponding to base 491–1201 of NM_001034818). PCR technology was used to amplify the coding sequence of *ggLin28B* from chick E5 ciliary ganglia and to fuse in front the Kozak sequence of the src oncogene. The fusion product was ligated into the expression vector pCAGGS using additional SacI and SphI sites of the polylinker (*ggLin28B* primer, sense, 5′-TTG AGC TCA CCA CCA TGG CCG AAG C-3′; antisense, 5′-TTG CAT GCT TAA GTT TTT TTC CTT TTC TGA ACA GAA GGC C-3′). Nonradioactive *in situ* hybridization (ISH) on cryosections was performed as described previously (Ernsberger et al., 1997) with the following modifications: hybridization was performed at 68°C, the following washing step was done at 72°C for at least 1.5 h. Sections were blocked for 2 h, and the anti-DIG antibody was applied in a dilution of 1:4500. ISH on mouse tissues was performed as described previously (Stubbusch et al., 2014). The following cRNA probes were used: *mmPhox2b* (1604 bp), *mmDbh* (987 bp; both kindly provided by J.-F. Brunet, Ecole Normale Superieure, Paris, France), and *mmNf-m* (680 bp, corresponding to base 2468-3147 of NM_008691). Images were taken using a Zeiss Axiophot2 microscope in combination with a Visitron systems spot RT3 camera, adapted for brightness and assembled in Photoshop.

For morphometric analysis, the area of *Dbh*, *Phox2b*, and *Nf-m* expression was imaged at 20× magnification. The areas were quantified using the MetaVue (version 7.1.3.0) imaging system. The stained areas were manually thresholded and quantified as square millimeters per section. The mean volume of ganglia and adrenal medulla was calculated using the Cavalieri principle (Gundersen et al., 1988). For statistical analysis unpaired two-tailed Student's *t* test was used.

qRT-PCR analysis. For expression analysis of *Lin28B* and the miRNA *Let-7a*, sympathetic ganglia from chicken embryos E6.5 to E12 were dissected, and RNA was isolated using the RNeasy Kit (Qiagen) for *Lin28B* and the miRNeasy Kit (Qiagen) for *Let-7a*, following the manufacturer's instructions. For the transcription of RNA into cDNA the SuperScript III reverse transcriptase (Invitrogen) was used for *Lin28B*, and the miScript II RT Kit (Qiagen) for *Let-7a*. For qPCR experiments of transfected neuroblasts, cells were plated on poly-DL-ornithine/laminin-coated 3.5 cm culture dishes in SG medium. After 2 d of cultivation, the cells were scraped off, and RNA/miRNA was isolated as described for dissected ganglia. qPCR experiments were performed using the QuantiTect SYBR Green PCR Kit with the following QuantiTect primer assays (Qiagen): *Gg_Lin28B_1_SG, Gg_Prox1_1_SG, Gg_Ntrk1_1_SG, Gg_Tfap2a_1_SG, Gg_Ascl1_1_SG*, and *Gg_Gapdh_1_SG*. For quantification of the miRNA *Let-7a*, the miScript SYBR Green PCR Kit in combination with miScript primer assays (Qiagen) for *Let-7a* (*Mm_let7a_2*) and *RNU (Hs_RNU6-2_11*) was used. The temperature profile for all qPCR experiments was the following: 95°C for 15 min and 40 cycles (94°C for 15 s, 55°C for 30 s, 72°C for 30 s). The primer pairs were analyzed for efficiency (>95%). At least triplets of every condition were performed in parallel. Data were normalized to *Gapdh* (mRNA) or *RNU6*(miRNA) as reference genes and evaluated using the $\Delta\Delta C_t$ method. Experiments were repeated independently at least three times and analyzed statistically using the pairwise fixed reallocation randomization test of relative expression software tool (REST; Pfaffl et al., 2002). For expression analysis of *Lin28B* and the miRNA *Let-7a* in mouse tissues, the same protocol was followed using the QuantiTect primer assays (Qiagen) *Mm_Lin28b_1_SG* and *Mm_Gapdh_3_SG*. Superior cervical ganglia (SCGs), stellate ganglia (STGs), and adrenal glands were dissected from postnatal day 0 (P0), P15–P20, and P60 mice as indicated. Tumors located at the adrenal gland or at the paravertebral sympathetic chain were dissected from P60–P100 mice.

Mice. LSL-Lin28B mice (Molenaar et al., 2012) and *Dbh-iCre* mice (Stanke et al., 2006; Parlato et al., 2007) have been described previously. *LSL-Lin28B* and *Dbh-iCre* mice backcrossed to 129X1/SvJ mice (Jackson Laboratory) were used. *LSL-Lin28B* mice were kept homozygous for the floxed *LSL-Lin28B* allele and crossed with heterozygous *Dbh-iCre* mice carrying an *iCre* recombinase transgene under control of the *dopamine β-hydroxylase* (*Dbh*) promoter, resulting in double-transgenic *LSL-Lin28B*^{DbhiCre} mice. *LSL-Lin28B* mice are used as controls. *TH-MYCN* mice backcrossed to 129/S2 were used (Weiss et al., 1997). Day of birth was counted as P0.

Dissection and fixation conditions for mouse tissues. For *in situ* hybridization and immunohistochemistry, P20 SCGs and adrenal glands dissected with adjacent connective tissue from mice of either sex were fixed with 4% (w/v) paraformaldehyde in 0.1 M sodium phosphate buffer, pH 7.4, at 4°C for 24 h. P0 mice, after removing the intestine, were fixed under the same conditions. Fixative was replaced by 30% (w/v) sucrose in 0.1 M sodium phosphate buffer, pH 7.4, for 24 h. Tissues were frozen in Tissue Tek (Sakura Finetek) and stored at −20°C. P22 STGs from *LSL-Lin28B* mice and P20 SCGs from *TH-MYCN* mice for Phox2b/Th and Ki67/Th double staining were embedded in Tissue Tek and frozen immediately after dissection. Twelve micrometer serial frozen sections were cut on a Leica CM3050 S cryostat. For RNA isolation, SCGs, STGs, and adrenal glands were dissected at P0 and P15–P19 and cleaned from connective tissue using a Leica Stereomicroscope.

Immunostaining. For immunostaining of mouse tissues, cryosections of either paraformaldehyde-fixed or unfixed tissues were used. Unfixed cryosections were postfixed with 4% paraformaldehyde (w/v) in 0.1 M sodium phosphate buffer, pH 7.4, at RT for 25 min. Fixed and postfixed cryosections were washed with PBS, followed by antigen retrieval by treating the sections with 100 mM sodium citrate, pH 6.0, at 95°C for 30 min. Sections were washed in H_2O and PBS. For Ki67/Th double staining, sections were incubated in PBS/0.1% Triton X-100 (w/v) for 10 min followed by washing steps with PBS. Blocking was performed with PBS/5% FCS (v/v)/1% BSA (w/v) for 60 min. The primary antibodies rat anti-mouse Ki-67 (BioLegend, clone 16A8, catalog #652402, 1:200), mouse anti-Th (1:100; Rohrer et al., 1986) and mouse anti-Islet1 (1:40) were diluted in blocking solution. The anti-Islet1 antibody 39.4D5 developed by T. Jessell (Columbia University, New York) was obtained from the Developmental Studies Hybridoma bank developed under the auspices of the NICHD and maintained by the University of Iowa Department of Biology (Iowa City, Iowa). Sections were incubated overnight at 4°C. After washing in PBS, Alexa 488 goat anti-mouse and Alexa 546 goat anti-rat antibodies were used as secondary antibodies. For detection of Phox2b sections were blocked with PBS/10% FCS (v/v)/1% BSA (w/v)/0.1% Triton X-100 (w/v) after antigen retrieval. The primary antibodies rabbit anti-mouse Phox2b (Pattyn et al., 1997) and mouse anti-Th (Rohrer et al., 1986) were used at 1:1000 and 1:100, respectively, in blocking solution. After washing in PBS/0.1% Triton X-100 (w/v), Alexa 488-conjugated goat anti-mouse and Alexa 594-conjugated goat anti-rabbit antibodies were used as secondary antibodies.

Results

Expression of Lin28B and Let-7 during sympathetic neuron development

The expression and function of *Lin28B* and *Let-7* during neuron generation was initially studied using embryonic stem (ES) cells and P19 embryocarcinoma (EC) cells induced to neuron differentiation (Wulczyn et al., 2007; Rybak et al., 2008). In these cells, *Let-7* expression is absent at the stem cell stage and is rapidly induced in differentiating neurons. *Lin28* shows a mirror image expression; i.e., it is present in ES and EC cells and decreases during differentiation. Neural stem and progenitor cells, in con-

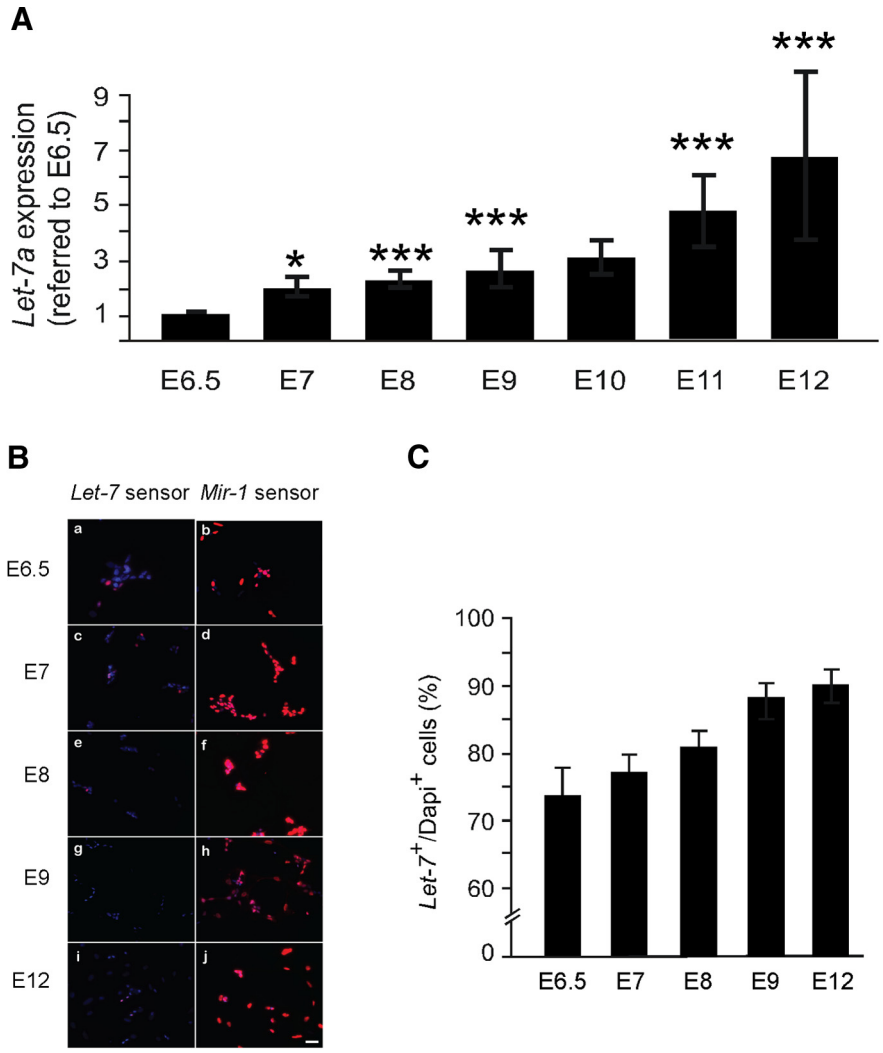

Figure 3. Analysis of *Let-7a* expression in developing chick sympathetic ganglia by qRT-PCR and by a *Let-7* sensor. ***A***, Expression of mature *Let-7* miRNA (normalized to *RNU6*) was quantified by qRT-PCR, using stem-loop primers. *Let-7a* expression levels were significantly increased from E8 onward compared to E6.5 levels (mean ± SEM; $n = 3$; statistical analysis by relative expression software REST). $*p < 0.05$; $***p < 0.001$. ***B***, ***C***, To determine *Let-7* expression at the single-cell level, freshly dissociated sympathetic ganglion cells were transfected with *Let-7* sensor RNA and *Mir-1* sensor RNA as control. We found that 75 ± 5% (mean ± SEM; $n = 3$) of transfected E6.5 sympathetic neuroblasts express *Let-7*, which is reflected by the degradation of the *Let-7* sensor RNA. Scale bar, 30 μm. ***C***, The percentage of *Let-7*-expressing cells increases with development, reaching 90 ± 2% (mean ± SEM; $n = 3$) at E12. The data were corrected for the RNA transfection efficiency (92 ± 2.6%). The *Mir-1* sensor RNA is maintained, demonstrating that degradation of sensor RNA depends on the presence of miRNA.

trast, express both *Let-7* and Lin28, and the developmental increase in *Let-7* levels was shown to control the temporal identity of retinal progenitors (Rybak et al., 2008; La Torre et al., 2013). In differentiated neurons, *Let-7* expression is maintained, but *Lin28* expression is lost. During neurogenesis in sympathetic ganglia neural progenitor cells differentiate to neuroblasts expressing catecholaminergic and neuronal properties. Neuroblasts continue to proliferate, and postmitotic neurons are produced by neuroblast cell cycle withdrawal (Rohrer, 2011). The restriction of *Lin28* expression to early progenitors in the retina (La Torre et al., 2013) suggested that *Lin28* expression would be limited to sympathetic progenitor cells present in the chick model only up to E5 (Tsarovina et al., 2008). Interestingly, *Lin28B* expression was detected by *in situ* hybridization in sympathetic ganglia up to E11 (Fig. 1). Although expression was highest at E4–E6, it was not restricted to neuron progenitor cells identified by *Notch1* expression, but rather present throughout the ganglion neuroblast/neuron population identified by *SCG10* expression (Fig. 1). Notably, also in the spinal cord, *Lin28B* expression is detectable in postmitotic neurons, most evident for motoneurons (data not shown). Similar expression patterns were observed for *Lin28A* in sympathetic ganglia and spinal cord (Fig. 1*A*; data not shown). The quantification of *Lin28B* in sympathetic ganglia by qRT-PCR demonstrates a significant decrease between E6.5, the earliest stage chick sympathetic ganglia can be dissected and E8 (Fig. 2). From E8 onward, the expression remains reduced, in the range of 20–40% of E6.5 levels.

Let-7 expression was followed using qRT-PCR for *Let-7a*, commonly used as a representative member of the *Let-7* family (Viswanathan et al., 2009; Molenaar et al., 2012; Nguyen et al., 2014), and revealed a steady strong (sixfold) increase in *Let-7a* expression between E6.5 and E12 (Fig. 3*A*). This result may reflect an increase in the proportion of *Let-7a*-expressing cells or a general increase in *Let-7a* levels in sympathetic neuroblasts. To address this issue, *Let-7* expression was analyzed at the cellular level using short-term cultures of sympathetic ganglion cells transfected with a *Let-7* sensor (La Torre et al., 2013). The sensor consists of RNA coding for a fluorescent protein (GFP) and contains *Let-7* binding sites in the 3-terminal UTR. In the absence of *Let-7*, transfected cells produce a strong fluorescent signal, whereas sensor RNA interacting with *Let-7* is rapidly degraded. At E6.5, when *Let-7a* levels are low (Fig. 3*A*), already 74 ± 5% of sympathetic neuroblasts express sufficient amounts of *Let-7* to degrade the sensor (Fig. 3*B*, *C*). The fraction of *Let-7*-expressing cells further increases and reaches 90 ± 2% at E12. The *miR-1* sensor, which was used as control because *miR-1* is not expressed in neurons, is not degraded (Fig. 3*B*). The increase in the fraction of *Let-7*-expressing cells cannot account for the sixfold increase in *Let-7a* levels, arguing for a general increase in *Let-7a* levels of sympathetic neuroblasts and neurons during development.

Lin28A and Lin28B are crucial for sympathetic neuroblast proliferation

The developmental changes in *Lin28A/B* and *Let-7a* expression levels do not correlate with the differentiation of sympathetic progenitor cells to noradrenergic neuroblasts, which terminates at E5 (Tsarovina et al., 2008), but are compatible with a function in neurogenesis, which extends between E3 and E12 in chick sympathetic ganglia (Rohrer, 2011; Holzmann et al., 2015). Maximal numbers of proliferating neuroblasts are present at E5–E7, decreasing to background levels at E12. To identify a role of *Lin28* in the control of proliferation, sympathetic neuroblasts were transfected *in vitro* with specific siRNA directed against *Lin28A* and *Lin28B*. Cultured neuroblasts from E7, E8, and E9 sympa-

thetic ganglia transfected with *siLin28A* and *siLin28B* display a strong reduction in the proportion of cells labeled with the S-phase marker EdU (Fig. 4*A*,*B*). The combined knockdown of both *Lin28A* and *Lin28B* did not further reduce proliferation, which is in agreement with a common target. These results demonstrate that Lin28A and Lin28B are important for the proliferation of sympathetic neurons and raise the questions of whether these effects may be due to reduced *Let-7* expression and whether the developmental increase of *Let-7* expression reflects an antiproliferative function.

Let-7 knockdown increases sympathetic neuroblast proliferation

To investigate the function of *Let-7* in neuroblast proliferation, sympathetic ganglion cells were transfected with a *Let-7* microRNA family inhibitor, which binds to and blocks all *Let-7* family members (Frost and Olson, 2011). Interfering with *Let-7* function increased neuroblast proliferation at E8 and E9, but did not quite reach significance at E7. The proportion of EdU^+ cells decreases in untreated controls from 43 ± 1.8% at E7 to 30 ± 2% at E8 and 25 ± 1.2% at E9 (Fig. 5). *Let-7* inhibition at E8 increased the proportion of EdU^+ cells to 41 ± 2.9%, comparable to the level observed in E7 controls. Similarly, at E9 the proportion of EdU^+ cells was increased upon *Let-7* inhibition to 34 ± 1.5%, close to the level observed in E8 control. These results indicate that the developmental increase in *Let-7* levels may contribute to the cell cycle withdrawal and termination of neurogenesis. The observation that the increase in proliferation elicited by *Let-7* inhibition at E7 does not reach significance ($p = 0.06$) suggests that the endogenous *Let-7* levels observed at this stage (Fig. 3) are not quite sufficient to repress neuroblast proliferation, in contrast to those at E8 and E9.

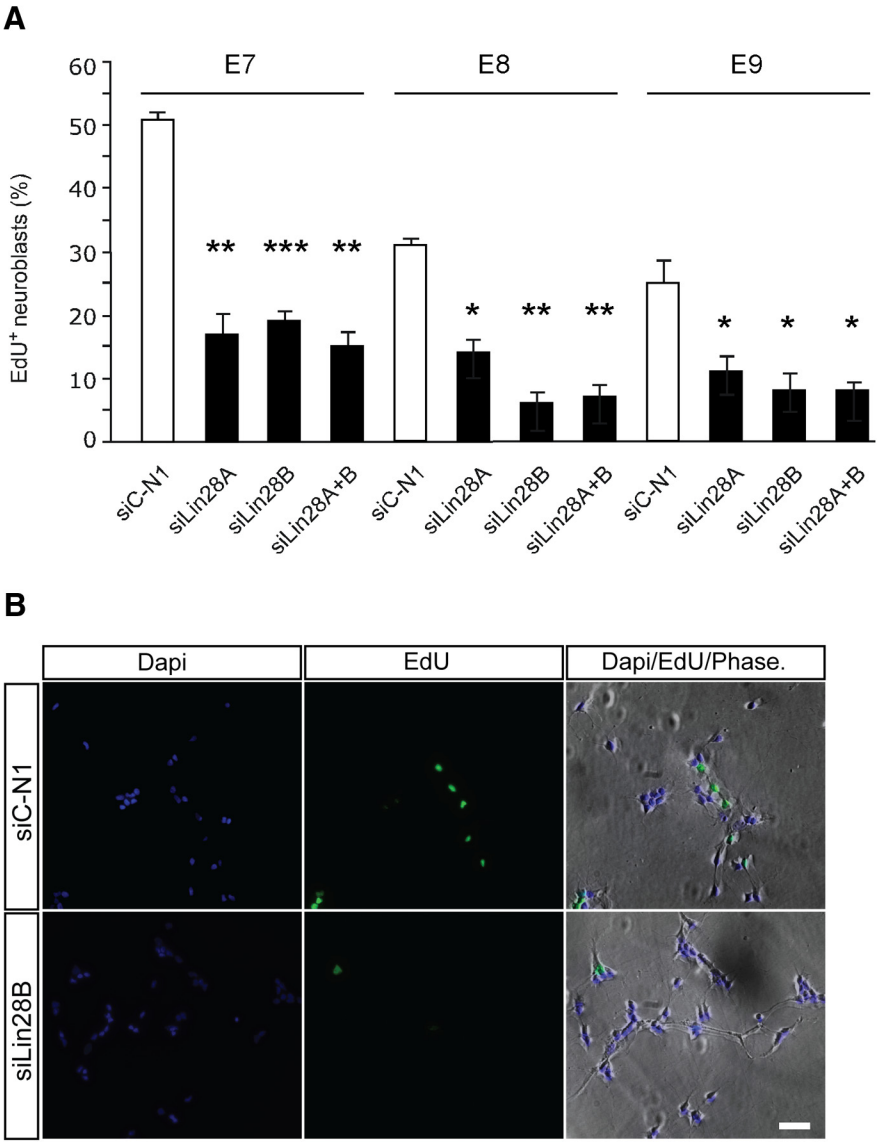

Figure 4. Proliferation of sympathetic neuroblasts depends on *Lin28A* and *Lin28B*. Freshly dissociated sympathetic ganglion cells from E7, E8, and E9 chick embryos were transfected with siRNA directed against *Lin28A*, *Lin28B*, or control *N1* siRNA and cultured for 2 d. ***A***, Proliferating neuroblasts were identified by EdU incorporation and quantified. Knockdown of *Lin28A* and *Lin28B* results in a significant reduction in sympathetic neuroblast proliferation at E7, E8, and E9 (mean ± SEM; $n = 3$). *$p < 0.05$; **$p < 0.01$; ***$p < 0.001$. ***B***, Cultures of E8 sympathetic ganglion cells transfected with *siC-N1* control and *siLin28B*. Nuclear DAPI staining, EdU-labeling, and combined DAPI, EdU, and phase contrast are shown to illustrate the reduced percentage of proliferating EdU^+ cells in cultures with *Lin28B* knockdown. Scale bar, 30 μm.

Lin28B overexpression increases sympathetic neuroblast proliferation

Lin28 and *Let-7* expression patterns and opposite functions of *Lin28* and *Let-7* in neuroblast proliferation are in agreement with the cross-regulatory expression of *Lin28* and *Let-7* observed in other lineages (Viswanathan et al., 2009; Thornton and Gregory, 2012). To support this notion, the effect of *Lin28B* overexpression was also investigated. Interestingly, increased proliferation was elicited by forced *Lin28B* expression only in E8 sympathetic neuroblasts, but not when E7 or E9 neuroblasts were transfected (Fig. 6*A*). Notably, *Let-7a* levels were not significantly reduced by *Lin28B* overexpression at all developmental stages investigated (Fig. 6*B*). In addition, *Let-7a* expression was unaffected by *Lin28A* or *Lin28*B knockdown at E8 (*Let-7a* expression in *Lin28A* knockdown, 1.7 ± 0.8; in *Lin28B* knockdown, 1.16 ± 0.15 compared to controls; mean ± SEM, $n = 3$–4). Thus, the proliferation effect in E8 neuroblasts cannot be explained by a selective effect on *Let-7a* expression. Developmental timing controlled by Lin28 involves two separate pathways, only one of which involves *Let-7* (Balzer et al., 2010; Vadla et al., 2012). To test the idea that *Lin28B* overexpression, although not reducing *Let-7* levels, may affect the timing of neuroblast development, markers for sympathetic progenitors and early neuroblasts (*Ascl1*, *AP-2a*, *Prox1*) and for more mature sympathetic neuroblasts and neurons (*TrkA*) were analyzed (Guillemot and Joyner, 1993; Von Holst et al., 1997; Schmidt et al., 2011; Holzmann et al., 2015). The expression levels of *Ascl1*, *AP-2a*, and *TrkA* are not changed by *Lin28B* overexpression, arguing against *Lin28B*-induced dedifferentiation (Fig. 6*C*). The reduction in *Prox1*, which is selectively

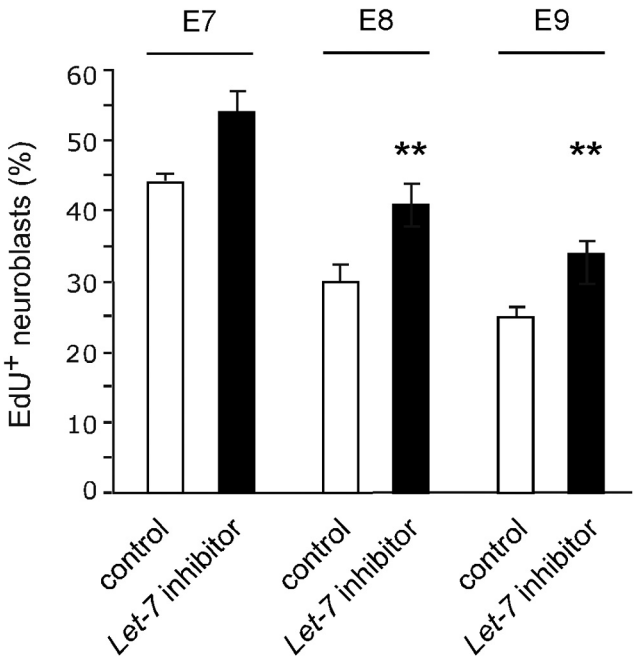

Figure 5. Proliferation of sympathetic neuroblasts is repressed by *Let-7*. Sympathetic ganglion cells from E7, E8, and E9 chick embryos were treated with a *Let-7* family inhibitor or a negative control inhibitor and analyzed for the proportion of EdU $^+$ proliferating cells after 2 d in culture. *Let-7* inhibition results in significantly increased proliferation at E8 and E9. The increase observed at E7 did not quite reach significance ($p = 0.06$; mean ± SEM; $n = 3–4$).

expressed in proliferating neuroblasts (Holzmann et al., 2015), may be explained by the decreased fraction of neuroblasts in the cell cycle.

In vivo effects of *Lin28B* overexpression in sympathetic ganglia and adrenals of the *LSL-Lin28B^{DBHiCre}* mouse line

To assess whether overexpression of *Lin28B* in noradrenergic cells can drive tumorigenesis, a transgenic mouse line was engineered in which *Lin28B* was introduced into the *Rosa26* locus under the control of the *CMV/β-actin* promotor (Molenaar et al., 2012). Because *Lin28B* expression is prevented by a stop codon flanked by two loxP sites (LSL), these mice are termed *LSL-Lin28B*. *LSL-Lin28B* mice were crossed with *DBHicre* mice (Stanke et al., 2006; Parlato et al., 2007), and double-transgenic mice (*Lin28B^{DbhiCre}*) were bred, expressing *Lin28B* in *DBH*-expressing cells as a result of stop codon elimination. Previous studies demonstrated that floxed genes are efficiently eliminated in sympathetic ganglia of *DBHiCre* mice at E11.5 (Parlato et al., 2007; Tsarovina et al., 2010; Majdazari et al., 2013). *Lin28B^{DbhiCre}* mice develop neuroblastoma with reduced *Let-7* expression in ganglia and adrenals between postnatal day 35 and 66 (Molenaar et al., 2012). However, the initial effects of *Lin28B* overexpression on sympathetic neuroblast proliferation, *Let-7* expression, and the development of precancerous stages are not known. To begin to address these issues, we first analyzed STG volume in *LSL-Lin28B^{DBHiCre}* mice compared to *LSL-Lin28B* mice at P0. *LSL-Lin28B* tissues served as controls. Serial sections of P0 animals at the brachial region were processed for *in situ* hybridization using specific probes for *Phox2b*, the general marker of the autonomic nervous system; for the noradrenergic marker *Dbh*; and for the neuronal marker *Nf-m*. Interestingly, the ganglion volume, determined from morphometric quantification of *Phox2b*-stained ganglion areas, is not increased in *Lin28B^{DBHiCre}* mice (Fig. 7*A*,*B*). The expression levels of *Dbh* and *Nf-m* are also unaffected (Fig. 7*B*). The absence of morphological effects correlates with a normal level of *Let-7a* expression, although *Lin28B* is increased by about 12-fold (Fig. 7*C*,*D*). The proportion of cycling neuroblasts is not increased in P0 STGs of *LSL-Lin28B^{DBHiCre}* mice as shown by Ki67 staining (Fig. 7*E*,*F*). Thus, *in vivo Lin28B* overexpression does not affect *Let-7a* expression, ganglion size, and neuroblast proliferation in P0 sympathetic ganglia.

In the TH-MYCN NB mouse model, precancerous lesions significantly increase between P0 and P14 in prevertebral ganglia (Hansford et al., 2004; Alam et al., 2009). To test whether *Lin28B* overexpression also affects sympathetic ganglion development during this period, *LSL-Lin28B^{DbhiCre}* mice were analyzed at P15 and P20. However, also at this stage, sympathetic ganglia of *LSL-Lin28B^{DbhiCre}* and control mice display similar ganglion volume (Fig. 8*A*) and *Let-7a* expression levels (*C*), although *Lin28B* expression levels are 17-fold higher than in control ganglia (*B*). *Let-7a* expression in sympathetic ganglia was maximally reduced to 30% in 1 out of 16 mice analyzed. *Lin28B* and *Let-7a* expression was also quantified in ganglionic tumors dissected from P60–P100 *Lin28B^{DBHiCre}* mice. In contrast to postnatal ganglia, *Let-7a* levels are massively reduced in *Lin28B*-induced ganglionic tumors compared to adult sympathetic ganglia from P60 *LSL-Lin28B* control mice (Fig. 8*E*). *Lin28B* expression levels are increased 26-fold (Fig. 8*D*).

The majority of primary human NB is located in the adrenal (Brodeur, 2003), and this pattern is recapitulated in *LSL-Lin28B^{DBHiCre}* mice (Molenaar et al., 2012). Thus, it was of interest to investigate adrenal medulla size and *Lin28B* and *Let-7* expression during postnatal development in *LSL-Lin28B^{DBHiCre}* mice and for comparison in *LSL-Lin28B^{DBHiCre}* adrenal tumors. The adrenal medulla volume, determined from *Dbh*-stained serial sections, was slightly increased at P0, but not at P20 (Fig. 9*A*–*C*). Similar to sympathetic ganglia, *Lin28B* was increased (Fig. 9*D*), but *Let-7a* expression was not affected in adrenals at P15 (Fig. 9*E*), but strongly reduced in adrenal tumors (*G*), which correlated with the very high *Lin28B* levels (*F*).

Together, these data demonstrate that elevation of *Lin28B* levels in *DBH*-expressing sympathetic neuroblasts and chromaffin cells neither affect *Let-7* expression nor tissue size and cell proliferation up to 2 weeks postnatally. In contrast, tumors that develop later in ganglia and adrenals display strongly reduced *Let-7a* levels and are highly proliferative (Molenaar et al., 2012; present findings).

Proliferation effects of *Lin28B* overexpression in sympathetic ganglia and adrenals of the *LSL-Lin28B^{DBHiCre}* mouse line

The strong difference in *Let-7a* expression observed between *Lin28B*-overexpressing P0–P20 sympathetic neurons and primary NB at ganglionic and adrenal locations may be explained by tumor initiation after P20 or by *Lin28B*-induced *Let-7* knockdown and proliferation in a small number of neuroblasts that remain undetected in our analysis. The latter scenario is realized in the *TH-MYCN* mouse where clusters of proliferating Phox2b $^+$/TH $^-$ neuroblasts are present in P0 ganglia of control and *TH-MYCN* mice in similar numbers, but are selectively maintained in MYCN-expressing ganglia (Hansford et al., 2004; Alam et al., 2009). Using double immunostaining for Phox2b and Th, we now demonstrate clusters of Phox2b $^+$ neuroblasts in SCGs of both *LSL-Lin28B^{DBHiCre}* and *LSL-Lin28B* controls at P0 (Fig. 10*A*). However, at P20, such cells are no more present in *Lin28B* overexpressing ganglia (Fig. 10*Ba–Bd*; $n = 10$) and control ganglia ($n = 3$; data not shown). Sympathetic ganglia of P22 *LSL-Lin28B^{DBHiCre}* mice were also devoid of clusters of prolifer-

ating Ki67$^+$ neuroblasts (Fig. 10*Ca–Cd*; $n = 8$). In contrast, clusters of cells with high Phox2b expression (Fig. 10*Be–Bh*) and Ki67$^+$ cell clusters (Fig. 10, *Ce–Ch*) are readily detected at P20 in *TH-MYCN* mice. This suggests that tumor initiation in *Lin28B*^{DbhiCre} mice differs from that in the *TH-MYCN* mouse model and does not involve the maintenance of proliferating precancerous cells.

Discussion

Forced expression of *Lin28B* in embryonic sympathetic neuroblasts results in NB that display reduced *Let-7* levels (Molenaar et al., 2012). Maintained proliferation of mouse JoMa1 neuroblasts in response to *Lin28B* overexpression suggested that NB evolves from the expansion of neuroblasts that fail to leave the cell cycle (Molenaar et al., 2012). We now document the expression of *Lin28A/B* and *Let-7a* during neurogenesis in chick sympathetic ganglia and demonstrate that neuroblast proliferation is maintained by *Lin28A/B* and repressed by *Let-7*. Unexpectedly, forced *Lin28B* expression does not affect *Let-7a* and has limited proliferation effects in cultured neuroblasts. Also in the *Lin28B*-overexpressing *LSL-Lin28B*^{DBHiCre} mouse line, sympathetic ganglia and adrenal medulla size and proliferation are not increased up to P20 and show normal *Let-7a* levels. These present findings demonstrate that NB does not evolve from expanding proliferating neuroblasts with reduced *Let-7* expression. Lin28B-induced tumor formation seems to require cooperation with additional signals activated in tumor founder cells at late postnatal stages.

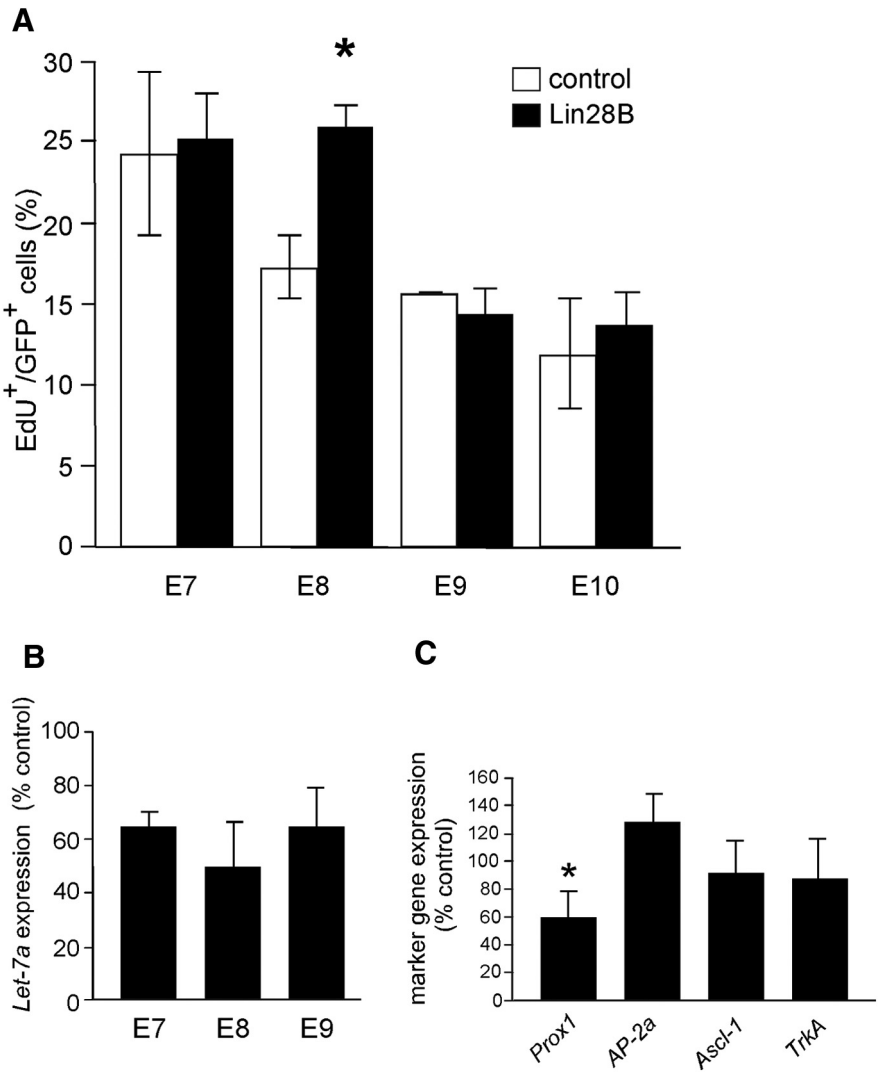

Figure 6. Overexpression of *Lin28B* increases proliferation of E8 neuroblasts, but does not affect *Let-7a* expression. ***A***, Forced expression of *Lin28B* in sympathetic neuroblasts increases the fraction of proliferating neuroblasts in cultures of E8, but not of E7, E9, and E10 ganglia. ***B***, *Let-7a* expression is not significantly affected by *Lin28B* overexpression at all ages analyzed ($p = 0.236$, 0.232, and 0.335 for E7, E8, and E9, respectively). ***C***, Forced expression of *Lin28B* in E8 neuroblasts results in reduced *Prox1* expression ($^*p < 0.05$), but does not affect *Ascl1*, *AP-2a*, and *TrkA* ($p = 0.034$, 0.83, 0.71, and 0.5 for *Prox1*, *Ascl1*, *AP-2a*, and *TrkA*, respectively; qRT-PCR analysis, mean ± SEM; $n = 3–6$; statistical analysis by REST).

Lin28A/B and Let-7 expression in developing sympathetic ganglia

Lin28A and *Lin28B* are expressed in a variety of developing tissues, including the nervous system. In the mouse neural tube, *Lin28A* is coexpressed with Sox2 at E9.5, but is lost at E10.5, although neural progenitor cells are present up to E13.5 (Helms and Johnson, 2003; Balzer et al., 2010). In the mouse retina, *Lin28B* is transiently expressed in early progenitors, and in cerebral cortex, overlapping expression of *Lin28A* and *Lin28B* was observed in nestin- and Pax6-expressing neural progenitor cells of the ventricular/subventricular zone (La Torre et al., 2013; Yang et al., 2015). In chick sympathetic ganglia, *Lin28A* and *Lin28B* expression is not restricted to progenitor cells, identified by *Notch1* expression (Tsarovina et al., 2008), but is also present in differentiated neuroblasts and maintained at reduced levels in postmitotic neurons. Low-level expression *of Lin28A/B* in differentiated neurons has been detected in rat and zebrafish spinal cord (Ramachandran et al., 2010; Yue et al., 2014). Notably, *Lin28* expression is also maintained in a number of differentiated tissues such as cardiac and skeletal muscle (Yang and Moss, 2003).

Let-7 expression in sympathetic ganglia was analyzed by qRT-PCR for *Let-7a* and by using a *Let-7* sensor. *Let-7a*, commonly used as representative member of the *Let-7* family (Viswanathan et al., 2009; Molenaar et al., 2012), is detectable at E6.5, the earliest time point sympathetic ganglia can be dissected in the chick embryo. During neurogenesis, *Let-7a* expression continuously increases up to E12, when the ganglia are mainly composed of postmitotic sympathetic neurons (Holzmann et al., 2015). Transfection of sympathetic ganglion cells with a *Let-7* sensor revealed that already at E6.5, 74 ± 5% of neuroblasts contained sufficient levels of *Let-7* to degrade the sensor RNA. The sixfold increase in *Let-7a* expression observed by qRT-PCR thus reflects increased expression per cell rather than an increase in the number of *Let-7*-expressing cells.

Lin28A/B and Let-7 function in developing sympathetic ganglia

The increase in *Let-7a* expression between E6.5 and E12 parallels the increase in the percentage of postmitotic neurons from 5 to 85% between E5 and E11 (Holzmann et al., 2015), suggesting that

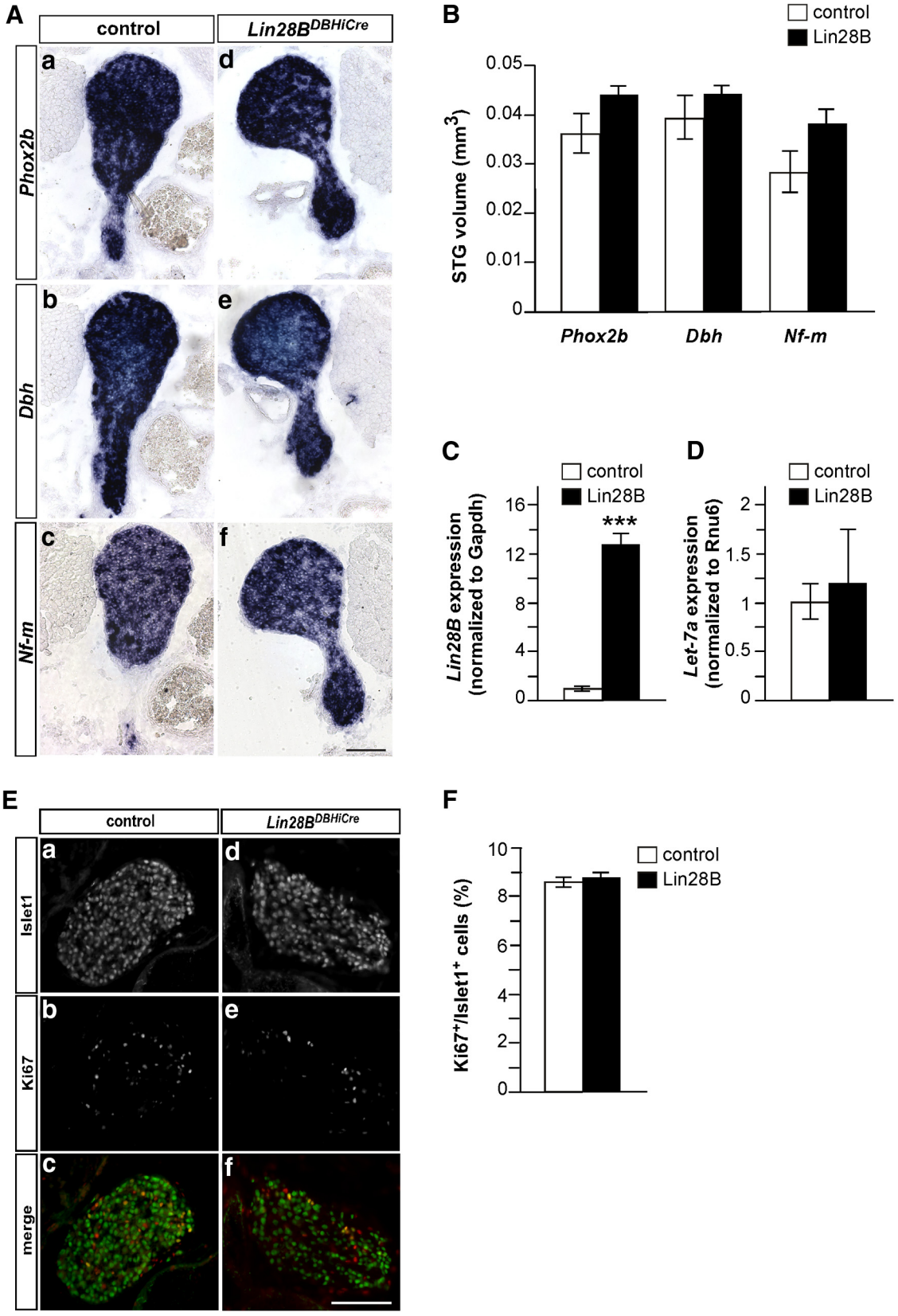

Figure 7. P0 sympathetic ganglia in *LSL-Lin28B*^{DbhiCre} mice display normal size, *Let-7* expression, and differentiation. ***A***, Sections from the brachial region (STG) of P0 control and *LSL-Lin28B*^{DbhiCre} mice were analyzed by *in situ* hybridization for the expression of *Phox2b, Dbh*, and *Nf-m*. ***B***, The STG volume was calculated from morphometric quantification of stained areas in serial sections (mean ± SEM; $n = 4$). ***C***, The expression level of *Lin28B* (normalized to *Gapdh*) in P0 STGs and SCGs was investigated by qRT-PCR and reveals a 12-fold increase in *LSL-Lin28B*^{DbhiCre} mice (mean ± SEM; $n = 10$ for *LSL-LIn28B*^{DbhiCre}; $n = 3$ for controls; statistical analysis by REST). ***$p < 0.001$. ***D***, qRT-PCR analysis of *Let-7a* expression (normalized to *RNU6*) in SCGs and STGs of control and *LSL-Lin28B*^{DbhiCre} mice (mean ± SEM; $n = 5$). ***E***, Identification of proliferating neuroblasts (Ki67^{+}/Islet1^{+}) in STGs of control and *LSL-Lin28B*^{DbhiCre} mice. ***F***, Quantification of Ki67^{+}/Islet1^{+} cells (mean ± SEM; $n = 4$). Scale bars, 100 μm.

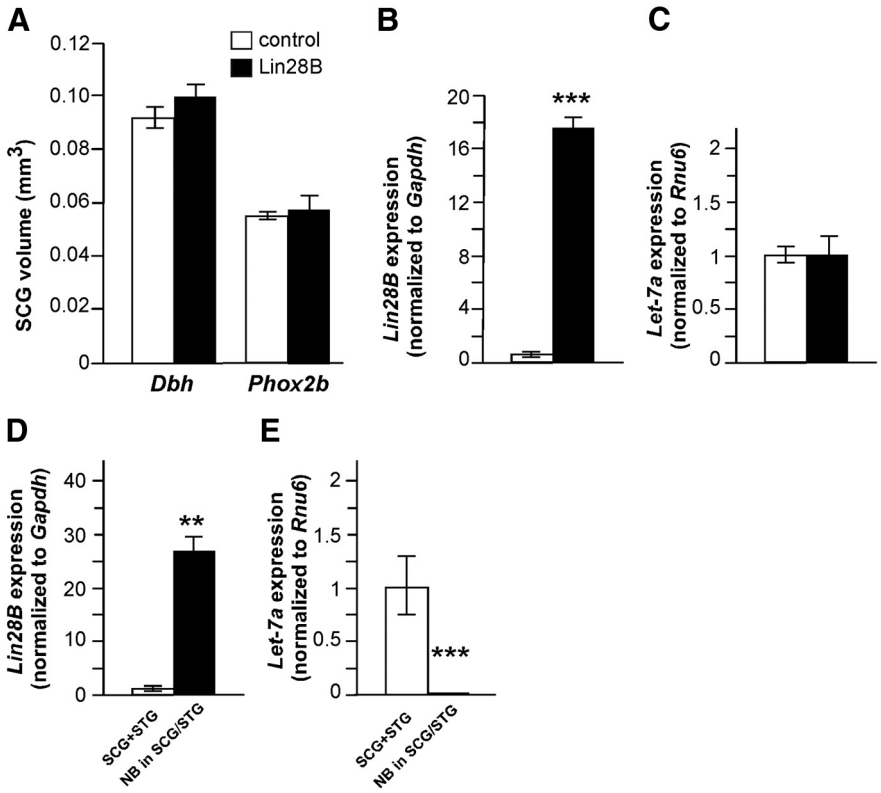

Figure 8. P15–P20 sympathetic ganglia in *LSL-Lin28B*^{DbhIcre} display normal size and *Let-7* expression, whereas *Lin28B*-induced ganglionic tumors are virtually devoid of *Let-7a*. ***A***, The SCG volume of *P20 LSL-Lin28B*^{DbhiCre} and control mice was calculated from morphometric quantification of *Phox2b*- and *Dbh*-stained areas in serial sections (mean ± SEM; control, $n = 3$; mutant, $n = 4$). ***B***, Quantification of *Lin28B* expression (normalized to *Gapdh*) in P15 STGs and SCGs by qRT-PCR reveals a 17-fold increase in *LSL-Lin28B*^{DbhiCre} mice compared to controls (mean ± SEM; $n = 5$; statistical analysis by REST). ***$p < 0.001$. ***C***, qRT-PCR analysis of *Let-7a* expression (normalized to *RNU6*) in P15 SCGs and STGs of control and *LSL-Lin28B*^{DbhiCre} mice (mean ± SEM; $n = 8$ for control; $n = 16$ for *LSL-Lin28B*^{DbhiCre}). ***D***, Quantification of *Lin28B* expression (normalized to *Gapdh*) in ganglionic tumors of P60–P100 *LSL-Lin28B*^{DbhiCre} mice by qRT-PCR reveals a 27-fold increase compared to P60 control (*LSL-Lin28B*) sympathetic ganglia (SCG+STG; mean ± SEM; $n = 5$; statistical analysis by REST). ***E***, qRT-PCR analysis of *Let-7a* expression in ganglionic tumors of P60–P100 *LSL-Lin28B*^{DbhiCre} mice compared to P60 sympathetic ganglia (SCG+STG) from *LSL-Lin28B* mice. *Let-7a* in NB is reduced to 0.005 ± 0.001 compared to control ganglia (mean ± SEM; $n = 5$; statistical analysis by REST). **$p < 0.01$; ***$p < 0.001$.

Let-7 interferes with cell proliferation as established in several other lineages (Schwamborn et al., 2009; Zhao et al., 2010). This notion was confirmed in sympathetic neuroblast cultures by the increase in proliferation resulting from *Let-7* inhibition. Lin28A and Lin28B, in contrast, are required for neuroblast proliferation, as blocking their expression by siRNA strongly reduces neuroblast proliferation. These experiments establish a function for endogenous Lin28 and *Let-7* in sympathetic neuron proliferation. It was expected from the cross-regulatory expression of *Let-7* and Lin28 in stem cells and tumor tissues (Viswanathan et al., 2009; Thornton and Gregory, 2012) that reduced proliferation upon Lin28 knockdown is caused by increased *Let-7* expression. Unexpectedly, Lin28B overexpression in cultured neuroblasts does not lead to the strong *Let-7* downregulation observed in many cell types, including neural stem cells (La Torre et al., 2013) and tumor cells (Viswanathan et al., 2009), nor is proliferation enhanced at all stages when endogenous *Lin28B* is required for proliferation. Only at one particular stage of development, E8, was increased proliferation observed in response to *Lin28B* overexpression. This result demonstrates that ectopically expressed Lin28B is functional and that Lin28B increases proliferation without significantly affecting *Let-7a* levels. Because Lin28 directly binds and influences the translation of a multitude of mRNAs including cyclins, cell cycle-dependent kinases, IGF-II, and glycolytic enzymes, Lin28 can directly potentiate cell proliferation and metabolism, independent of *Let-7* (Polesskaya et al., 2007; Xu et al., 2009; Graf et al., 2013; Hafner et al., 2013; Shyh-Chang and Daley, 2013). Notably, progenitor proliferation and prevention of cell cycle exit in the developing cerebral cortex does not involve *Let-7* (*Let-7a-d*), but rather Igf2-mTor signaling (Yang et al., 2015). Because IGFs have been shown previously to control sympathetic neuroblast proliferation (Zackenfels et al., 1995), we hypothesize that altered IGF signaling rather than *Let-7* expression may underlie the Lin28B effects.

But how can the timing of the effects of Lin28B overexpression to a particular stage of development be explained? If Lin28B acts as heterochronic gene and shifts the identity of neuroblasts toward earlier stages, an increased proliferation at E9 and E10 would be expected. A heterochronic function is also excluded by the finding that marker genes for progenitors and early neuroblasts (*Ascl1*, *AP-2a*, *Prox1*; Guillemot and Joyner, 1993; Schmidt et al., 2011; Holzmann et al., 2015) are not upregulated in response to *Lin28B* overexpression. A more likely explanation is that neuroblasts change their properties during neurogenesis, which is reflected by different sympathetic neuron phenotypes produced (Chubb and Anderson, 2010) and may also affect the response to *Lin28B* overexpression. Although the mechanisms that are responsible for the developmental restriction of *Lin28B* effects remain unclear, our findings allow the conclusion that *Lin28B* overexpression does not lead to a general prolongation of neuroblast proliferation and reduced *Let-7a* expression.

Lin28B function in the *LSL-Lin28B*^{DBHiCre} NB mouse model

Lin28 regulates the timing of differentiation of embryonic tissues and is upregulated in poorly differentiated tumors (Ambros and Horvitz, 1984; Moss et al., 1997; Viswanathan and Daley, 2010). This suggests a function for Lin28 in tumor development by maintaining stem and progenitor cells or by Lin28-induced dedifferentiation. Indeed, *Lin28A* overexpression has been implicated in pediatric tumor formation, which is caused by a failure of differentiation (Gillis et al., 2011; Urbach et al., 2014). Neuroblastoma elicited by forced *Lin28B* expression in noradrenergic neuroblasts was also considered to be due to progenitor maintenance and failed terminal differentiation (Marshall et al., 2014). Our present analysis of sympathoadrenal cells in a *Lin28B* overexpressing mouse line reveals that sympathetic ganglia and adrenal medulla are indistinguishable from controls with respect to tissue size, expression of differentiation markers, proliferation, and *Let-7a* expression up to P20, although the *Cre*-recombinase in *Lin28B*^{DBHiCre} animals is expected to initiate Lin28B expression at early embryonic stages (E11.5; Parlato et al., 2007; Tsar-

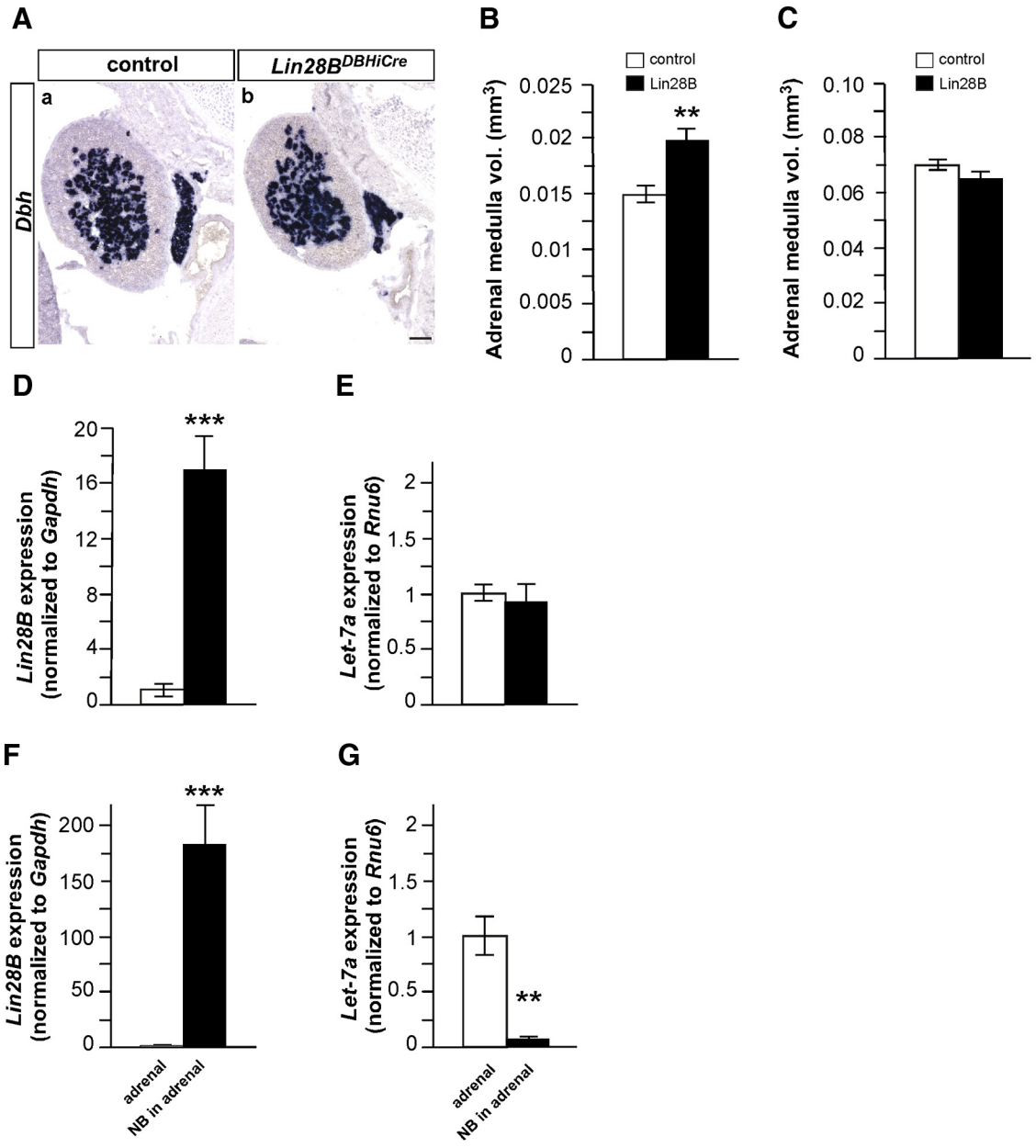

Figure 9. Adrenal medulla in *LSL-Lin28B*^{DbhiCre} mice display normal size and *Let-7* expression up to P20, whereas *Lin28B*-induced tumors show strongly reduced *Let-7a* expression. ***A***, Adrenals from P0 control and *LSL-Lin28B*^{DbhiCre} mice analyzed by *in situ* hybridization for *Dbh* expression. Scale bar, 100 μm. ***B***, P0 adrenal medulla volume calculated from *Dbh*-stained serial sections from *LSL-Lin28B*^{DbhiCre} and control mice (mean ± SEM; $n = 7$ for control; $n = 9$ for *LSL-Lin28B*^{DbhiCre}). ***C***, P20 adrenal medulla volume calculated from *Dbh*-stained serial sections does not differ between *LSL-Lin28B*^{DbhiCre} and controls (mean ± SEM; $n = 8$ for control; $n = 12$ for *LSL-Lin28B*^{DbhiCre}). ***D***, Quantification of *Lin28B* expression in P15/P16 adrenal glands by qRT-PCR reveals a 17-fold increase in *LSL-Lin28B*^{DbhiCre} mice (mean ± SEM; $n = 3$; statistical analysis by REST). ***E***, qRT-PCR analysis of *Let-7a* expression in P15/P16 adrenal glands of control and *LSL-Lin28B*^{DbhiCre} mice (mean ± SEM; $n = 5$). ***F***, Quantification of *Lin28B* expression in adrenal tumors of P60 –P100 *LSL-Lin28B*^{DbhiCre} mice by qRT-PCR reveals a 175-fold increase compared to P60 control adrenals (mean ± SEM; $n = 5$; statistical analysis by REST). ***G***, qRT-PCR analysis of *Let-7a* expression in adrenal tumors of P60 –P100 *LSL-Lin28B*^{DbhiCre} mice compared to P60 *LSL-Lin28B* control adrenals. *Let-7a* in NB is reduced to 0.07 ± 0.01 compared to control adrenals (mean ± SEM; $n = 5$; statistical analysis by REST). $^{**}p < 0.01$; $^{***}p < 0.001$.

ovina et al., 2010; Majdazari et al., 2013). Given that cultured sympathetic neuroblasts also show a limited proliferation response to *Lin28B*, we conclude that *Lin28B* overexpressison is not sufficient to maintain neuroblasts in the cell cycle. In addition, in both chick and mouse neuroblasts, *Lin28B* overexpression does not lead to decreased *Let-7a* levels.

These results suggest that the strongly reduced *Let-7* levels observed in ganglionic and adrenal tumors of *Lin28B*^{DBHiCre} mice may not be directly and exclusively linked to increased Lin28B levels in sympathetic neuroblasts. In addition, they raise the question as to the identity of Lin28B targets that eventually lead to NB development. Previous evidence suggests that mRNAs in addition to microRNAs are major Lin28 targets (Cho et al., 2012; Hafner et al., 2013). Direct targets of Lin28 with increased mRNA translation and/or stabilization include genes contributing to cell cycle regulation (e.g., CyclinD1/D2, Cyclin B1, Cdk1/2) and components of the IGF2-PI3K-mTor signaling pathway (Polesskaya et al., 2007; Xu et al., 2009; Yang et al., 2015). Given that mTOR signaling affects translation and stabilization of MYC proteins (West et al., 1998; Johnsen et al., 2008; Sun and Jin, 2008) and MYCN activates and sustains the mTOR pathway (Pourdehnad et al., 2013; Schramm et al., 2013; Moore et al., 2014), it is

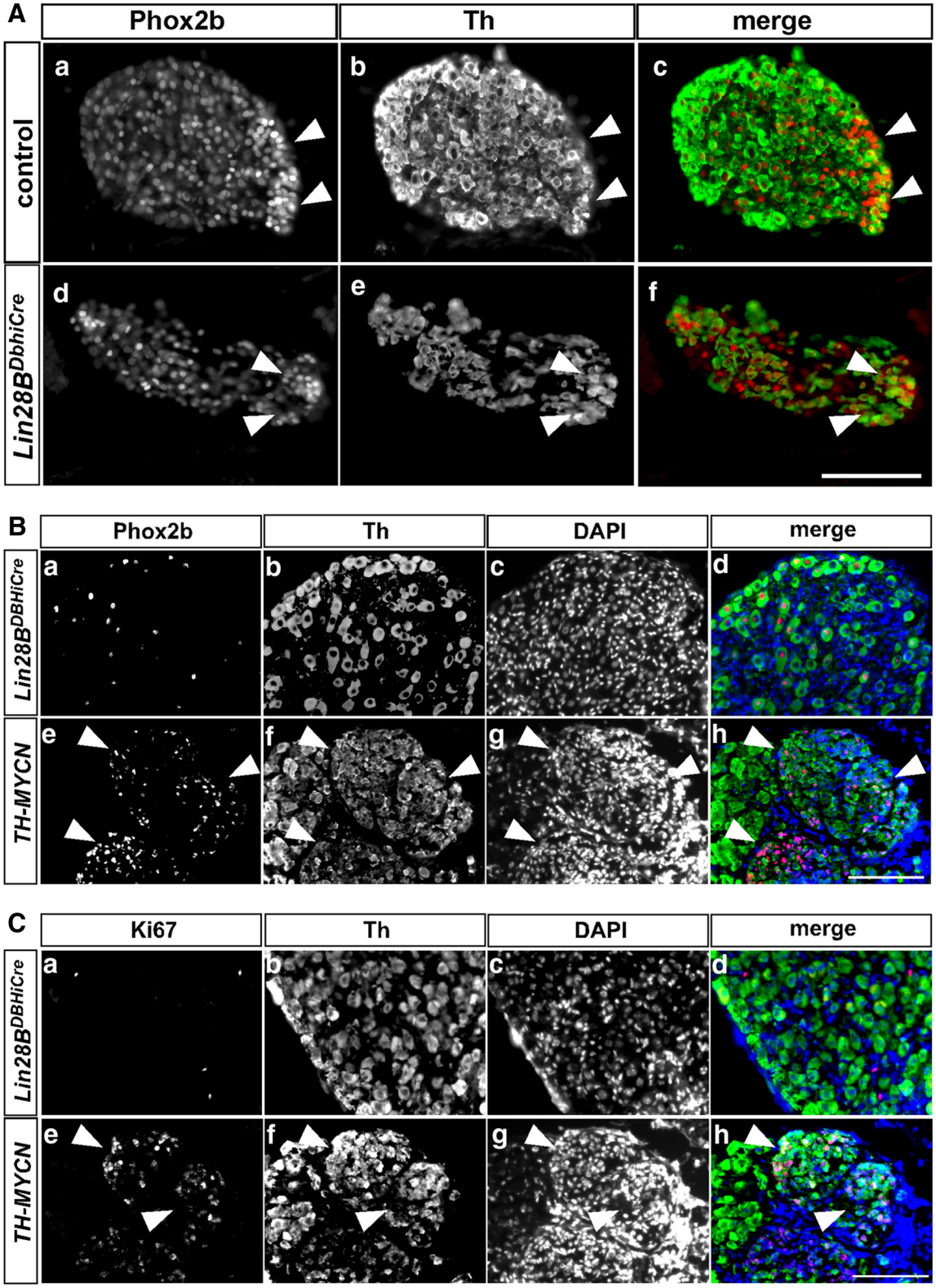

Figure 10. Clusters of proliferating Ki67 $^{+}$ and Phox2b $^{+}$ neuroblasts are not observed in sympathetic ganglia of *LSL-Lin28B*^{DbhiCre} at P20. ***A***, Double immunostaining for Phox2b and Th on frozen sections of P0 SCGs reveals clusters of Phox2b $^{+}$/Th $^{+}$ cells (arrowheads) in ganglia of both control and *LSL-Lin28B*^{DbhIcre} mice. ***B***, At P20–P22, clusters of Phox2b $^{+}$ cells are absent in *LSL-Lin28B*^{DbhIcre} SCGs ($n = 10$; ***a–d***) and controls ($n = 3$; data not shown), but present in *TH-MYCN* STGs (***e–h***, arrowheads). The absence of Phox2b immunoreactivity in cells outside of the clusters (***e***, in contrast to ***a***) is explained by different fixation conditions. ***C***, Ki67 $^{+}$ cells are scarce and show a scattered distribution in P22 STGs of *LSL-Lin28B*^{DbhIcre} (***a–d***; $n = 8$) and control ($n = 4$; data not shown) mice. Less than 1% of all DAPI $^{+}$ nuclei are Ki67 $^{+}$ in control and *LSL-Lin28B*^{DbhiCre} mice. In contrast, clusters of Ki67 $^{+}$ cells with low Th levels are detected in P20 SCGs of *TH-MYCN* mice (***e–h***, arrowheads). Scale bars, 100 μm.

tempting to speculate that NB initiation in postnatal *LSL-Lin28B*^{DbhiCre} mice may involve increased translation of IGF-2-mTor signal pathway components leading to an increase in MYCN protein. In tumors of adult *LSL-Lin28B*^{DbhiCre} mice, reduced *Let-7* expression contributes to the stabilization of endogenous MYCN, which drives tumor growth as shown by reduced tumor size upon treatment with the MYCN antagonist JQ-1 (Molenaar et al., 2012). Together, the present results argue against a role for *Let-7* and rather implicate other Lin28B targets during the initial stages of NB development.

References

Alam G, Cui H, Shi H, Yang L, Ding J, Mao L, Maltese WA, Ding HF (2009) MYCN promotes the expansion of Phox2B-positive neuronal progenitors to drive neuroblastoma development. Am J Pathol 175:856–866. CrossRef Medline

Ambros V, Horvitz HR (1984) Heterochronic mutants of the nematode *Caenorhabditis elegans*. Science 226:409–416. CrossRef Medline

Balzer E, Heine C, Jiang Q, Lee VM, Moss EG (2010) LIN28 alters cell fate succession and acts independently of the let-7 microRNA during neurogliogenesis *in vitro*. Development 137:891–900. CrossRef Medline

Brodeur GM (2003) Neuroblastoma: biological insights into a clinical enigma. Nat Rev Cancer 3:203–216. CrossRef Medline

Cho J, Chang H, Kwon SC, Kim B, Kim Y, Choe J, Ha M, Kim YK, Kim VN (2012) LIN28A is a suppressor of ER-associated translation in embryonic stem cells. Cell 151:765–777. CrossRef Medline

Chubb DP, Anderson CR (2010) The relationship of the birth date of rat sympathetic neurons to the target they innervate. Dev Dyn 239:897–904. CrossRef Medline

Diskin SJ, Capasso M, Schnepp RW, Cole KA, Attiyeh EF, Hou C, Diamond M, Carpenter EL, Winter C, Lee H, Jagannathan J, Latorre V, Iolascon A, Hakonarson H, Devoto M, Maris JM (2012) Common variation at 6q16 within HACE1 and LIN28B influences susceptibility to neuroblastoma. Nat Genet 44:1126–1130. CrossRef Medline

Ernsberger U, Patzke H, Rohrer H (1997) The developmental expression of choline acetyltransferase (ChAT) and the neuropeptide VIP in chick sympathetic neurons: evidence for different regulatory events in cholinergic differentiation. Mech Dev 68:115–126. CrossRef Medline

Frost RJ, Olson EN (2011) Control of glucose homeostasis and insulin sensitivity by the Let-7 family of microRNAs. Proc Natl Acad Sci U S A 108:21075–21080. CrossRef Medline

Gillis AJ, Stoop H, Biermann K, van Gurp RJ, Swartzman E, Cribbes S, Ferlinz A, Shannon M, Oosterhuis JW, Looijenga LH (2011) Expression and interdependencies of pluripotency factors LIN28, OCT3/4, NANOG and SOX2 in human testicular germ cells and tumours of the testis. Int J Androl 34:e160–e174. CrossRef Medline

Gonsalvez DG, Cane KN, Landman KA, Enomoto H, Young HM, Anderson CR (2013) Proliferation and cell cycle dynamics in the developing stellate ganglion. J Neurosci 33:5969–5979. CrossRef Medline

Graf R, Munschauer M, Mastrobuoni G, Mayr F, Heinemann U, Kempa S, Rajewsky N, Landthaler M (2013) Identification of LIN28B-bound mRNAs reveals features of target recognition and regulation. RNA Biol 10:1146–1159. CrossRef Medline

Guillemot F, Joyner AL (1993) Dynamic expression of the murine *Achaete-Scute* homologue *Mash-1* in the developing nervous system. Mech Dev 42:171–185. CrossRef Medline

Gundersen HJ, Bendtsen TF, Korbo L, Marcussen N, Møller A, Nielsen K, Nyengaard JR, Pakkenberg B, Sørensen FB, Vesterby A, West MJ (1988) Some new, simple and efficient stereological methods and their use in pathological research and diagnosis. APMIS 96:379–394. CrossRef Medline

Hafner M, Max KE, Bandaru P, Morozov P, Gerstberger S, Brown M, Molina H, Tuschl T (2013) Identification of mRNAs bound and regulated by human LIN28 proteins and molecular requirements for RNA recognition. RNA 19:613–626. CrossRef Medline

Hamburger V, Hamilton HL (1951) A series of normal stages in the development of the chick embryo. J Exp Zool 88:49–92.

Hansford LM, Thomas WD, Keating JM, Burkhart CA, Peaston AE, Norris MD, Haber M, Armati PJ, Weiss WA, Marshall GM (2004) Mechanisms of embryonal tumor initiation: distinct roles for MycN expression and MYCN amplification. Proc Natl Acad Sci U S A 101:12664–12669. CrossRef Medline

Helms AW, Johnson JE (2003) Specification of dorsal spinal cord interneurons. Curr Opin Neurobiol 13:42–49. CrossRef Medline

Holzmann J, Hennchen M, Rohrer H (2015) Prox1 identifies proliferating neuroblasts and nascent neurons during neurogenesis in sympathetic ganglia. Dev Neurobiol 12:1352–1367. CrossRef Medline

Johnsen JI, Segerström L, Orrego A, Elfman L, Henriksson M, Kågedal B, Eksborg S, SveinbjörnssonB, Kogner P (2008) Inhibitors of mammalian target of rapamycin downregulate MYCN protein expression and inhibit neuroblastoma growth *in vitro* and *in vivo*. Oncogene 27:2910–2922. CrossRef Medline

La Torre A, Georgi S, Reh TA (2013) Conserved microRNA pathway regulates developmental timing of retinal neurogenesis. Proc Natl Acad Sci U S A 110:E2362–E2370. CrossRef Medline

Majdazari A, Stubbusch J, Müller CM, Hennchen M, Weber M, Deng CX, Mishina Y, Schütz G, Deller T, Rohrer H (2013) Dendrite complexity of sympathetic neurons is controlled during postnatal development by BMP signaling. J Neurosci 33:15132–15144. CrossRef Medline

Maris JM, Hogarty MD, Bagatell R, Cohn SL (2007) Neuroblastoma. Lancet 369:2106–2120. CrossRef Medline

Marshall GM, Carter DR, Cheung BB, Liu T, Mateos MK, Meyerowitz JG, Weiss WA (2014) The prenatal origins of cancer. Nat Rev Cancer 14:277–289. CrossRef Medline

Molenaar JJ, Domingo-Fernández R, Ebus ME, Lindner S, Koster J, Drabek K, Mestdagh P, van Sluis P, Valentijn LJ, van Nes J, Broekmans M, Haneveld F, Volckmann R, Bray I, Heukamp L, Sprüssel A, Thor T, Kieckbusch K, Klein-Hitpass L, Fischer M, et al. (2012) LIN28B induces neuroblastoma and enhances MYCN levels via let-7 suppression. Nature Genet 44:1199–1206. CrossRef Medline

Moore NF, Azarova AM, Bhatnagar N, Ross KN, Drake LE, Frumm S, Liu QS, Christie AL, Sanda T, Chesler L, Kung AL, Gray NS, Stegmaier K, George RE (2014) Molecular rationale for the use of PI3K/AKT/mTOR pathway inhibitors in combination with crizotinib in ALK-mutated neuroblastoma. Oncotarget 5:8737–8749. CrossRef Medline

Moss EG, Lee RC, Ambros V (1997) The cold shock domain protein LIN-28 controls developmental timing in *C. elegans* and is regulated by the lin-4 RNA. Cell 88:637–646. CrossRef Medline

Nguyen LH, Robinton DA, Seligson MT, Wu L, Li L, Rakheja D, Comerford SA, Ramezani S, Sun X, Parikh MS, Yang EH, Powers JT, Shinoda G, Shah SP, Hammer RE, Daley GQ, Zhu H (2014) Lin28b is sufficient to drive liver cancer and necessary for its maintenance in murine models. Cancer Cell 26:248–261. CrossRef Medline

Parlato R, Otto C, Begus Y, Stotz S, Schütz G (2007) Specific ablation of the transcription factor CREB in sympathetic neurons surprisingly protects against developmentally regulated apoptosis. Development 134:1663–1670. CrossRef Medline

Pattyn A, Morin X, Cremer H, Goridis C, Brunet JF (1997) Expression and interactions of the two closely related homeobox genes *Phox2a* and *Phox2b* during neurogenesis. Development 124:4065–4075. Medline

Pfaffl MW, Horgan GW, Dempfle L (2002) Relative expression software tool (REST) for group-wise comparison and statistical analysis of relative expression results in real-time PCR. Nucleic Acids Res 30:e36. CrossRef Medline

Polesskaya A, Cuvellier S, Naguibneva I, Duquet A, Moss EG, Harel-Bellan A (2007) Lin-28 binds IGF-2 mRNA and participates in skeletal myogenesis by increasing translation efficiency. Genes Dev 21:1125–1138. CrossRef Medline

Pourdehnad M, Truitt ML, Siddiqi IN, Ducker GS, Shokat KM, Ruggero D (2013) Myc and mTOR converge on a common node in protein synthesis control that confers synthetic lethality in Myc-driven cancers. Proc Natl Acad Sci U S A 110:11988–11993. CrossRef Medline

Ramachandran R, Fausett BV, Goldman D (2010) Ascl1a regulates Muller glia dedifferentiation and retinal regeneration through a Lin-28-dependent, let-7 microRNA signalling pathway. Nat Cell Biol 12:1101–1107. CrossRef Medline

Reiff T, Huber L, Kramer M, Delattre O, Janoueix-Lerosey I, Rohrer H (2011) Midkine and Alk signaling in sympathetic neuron proliferation and neuroblastoma predisposition. Development 138:4699–4708. CrossRef Medline

Rohrer H (2011) Transcriptional control of differentiation and neurogenesis in autonomic ganglia. Eur J Neurosci 34:1563–1573. CrossRef Medline

Rohrer H, Thoenen H (1987) Relationship between differentiation and terminal mitosis: chick sensory and ciliary neurons differentiate after termi-

nal mitosis of precursor cells whereas sympathetic neurons continue to divide after differentiation. J Neurosci 7:3739–3748. Medline

Rohrer H, Acheson AL, Thibault J, Thoenen H (1986) Developmental potential of quail dorsal root ganglion cells analyzed *in vitro* and *in vivo*. J Neurosci 6:2616–2624. Medline

Rothman TP, Gershon MD, Holtzer H (1978) The relationship of cell division to the acquisition of adrenergic characteristics by developing sympathetic ganglion cell precursors. Dev Biol 65:321–341.

Rybak A, Fuchs H, Smirnova L, Brandt C, Pohl EE, Nitsch R, Wulczyn FG (2008) A feedback loop comprising lin-28 and let-7 controls pre-let-7 maturation during neural stem-cell commitment. Nat Cell Biol 10: 987–993. CrossRef Medline

Schmidt M, Huber L, Majdazari A, Schütz G, Williams T, Rohrer H (2011) The transcription factors AP-2beta and AP-2alpha are required for survival of sympathetic progenitors and differentiated sympathetic neurons. Dev Biol 355:89–100. CrossRef Medline

Schramm A, Köster J, Marschall T, Martin M, Schwermer M, Fielitz K, BüchelG, Barann M, Esser D, Rosenstiel P, Rahmann S, Eggert A, Schulte JH (2013) Next-generation RNA sequencing reveals differential expression of MYCN target genes and suggests the mTOR pathway as a promising therapy target in MYCN-amplified neuroblastoma. Int J Cancer 132:E106–E115. CrossRef Medline

Schwamborn JC, Berezikov E, Knoblich JA (2009) The TRIM-NHL protein TRIM32 activates microRNAs and prevents self-renewal in mouse neural progenitors. Cell 136:913–925. CrossRef Medline

Shyh-Chang N, Daley GQ (2013) Lin28: primal regulator of growth and metabolism in stem cells. Cell Stem Cell 12:395–406. CrossRef Medline

Stanke M, Duong CV, Pape M, Geissen M, Burbach G, Deller T, Gascan H, Otto C, Parlato R, Schütz G, Rohrer H (2006) Target-dependent specification of the neurotransmitter phenotype: cholinergic differentiation of sympathetic neurons is mediated *in vivo* by gp130 signaling. Development 133:141–150. CrossRef Medline

Stubbusch J, Narasimhan P, Hennchen M, Huber K, Unsicker K, Ernsberger U, Rohrer H (2014) Lineage and stage specific requirement for Dicer1 in sympathetic ganglia and adrenal medulla formation and maintenance. Dev Biol 400:210–223. CrossRef

Sun J, Jin T (2008) Both Wnt and mTOR signaling pathways are involved in insulin-stimulated proto-oncogene expression in intestinal cells. Cell Signal 20:219–229. CrossRef Medline

Thornton JE, Gregory RI (2012) How does Lin28 let-7 control development and disease? Trends Cell Biol 22:474–482. CrossRef Medline

Tsarovina K, Schellenberger J, Schneider C, Rohrer H (2008) Progenitor cell maintenance and neurogenesis in sympathetic ganglia involves Notch signaling. Mol Cell Neurosci 37:20–31. CrossRef Medline

Tsarovina K, Reiff T, Stubbusch J, Kurek D, Grosveld FG, Parlato R, Schütz G, Rohrer H (2010) The Gata3 transcription factor is required for the survival of embryonic and adult sympathetic neurons. J Neurosci 30:10833–10843. CrossRef Medline

Urbach A, Yermalovich A, Zhang J, Spina CS, Zhu H, Perez-Atayde AR, Shukrun R, Charlton J, Sebire N, Mifsud W, Dekel B, Pritchard-Jones K, Daley GQ (2014) Lin28 sustains early renal progenitors and induces Wilms tumor. Genes Dev 28:971–982. CrossRef Medline

Vadla B, Kemper K, Alaimo J, Heine C, Moss EG (2012) lin-28 controls the succession of cell fate choices via two distinct activities. PLoS Genet 8:e1002588. CrossRef Medline

Viswanathan SR, Daley GQ (2010) Lin28: A microRNA regulator with a macro role. Cell 140:445–449. CrossRef Medline

Viswanathan SR, Powers JT, Einhorn W, Hoshida Y, Ng TL, Toffanin S, O'Sullivan M, Lu J, Phillips LA, Lockhart VL, Shah SP, Tanwar PS, Mermel CH, Beroukhim R, Azam M, Teixeira J, Meyerson M, Hughes TP, Llovet JM, Radich J, et al. (2009) Lin28 promotes transformation and is associated with advanced human malignancies. Nat Genet 41:843–848. CrossRef Medline

Von Holst A, Lefcort F, Rohrer H (1997) TrkA expression levels of sympathetic neurons correlate with NGF-dependent survival during development and after treatment with retinoic acid. Eur J Neurosci 9:2169–2177. CrossRef Medline

Wakamatsu Y, Maynard TM, Weston JA (2000) Fate determination of neural crest cells by NOTCH-mediated lateral inhibition and asymmetrical cell division during gangliogenesis. Development 127:2811–2821. Medline

Weiss WA, Aldape K, Mohapatra G, Feuerstein BG, Bishop JM (1997) Targeted expression of MYCN causes neuroblastoma in transgenic mice. EMBO J 16:2985–2995. CrossRef Medline

West MJ, Stoneley M, Willis AE (1998) Translational induction of the c-myc oncogene via activation of the FRAP/TOR signalling pathway. Oncogene 17:769–780. CrossRef Medline

Wulczyn FG, Smirnova L, Rybak A, Brandt C, Kwidzinski E, Ninnemann O, Strehle M, Seiler A, Schumacher S, Nitsch R (2007) Post-transcriptional regulation of the let-7 microRNA during neural cell specification. FASEB J 21:415–426. CrossRef Medline

Xu B, Zhang K, Huang Y (2009) Lin28 modulates cell growth and associates with a subset of cell cycle regulator mRNAs in mouse embryonic stem cells. RNA 15:357–361. CrossRef Medline

Yang DH, Moss EG (2003) Temporally regulated expression of Lin-28 in diverse tissues of the developing mouse. Gene Expr Patterns 3:719–726. CrossRef Medline

Yang M, Yang SL, Herrlinger S, Liang C, Dzieciatkowska M, Hansen KC, Desai R, Nagy A, Niswander L, Moss EG, Chen JF (2015) Lin28 promotes the proliferative capacity of neural progenitor cells in brain development. Development 142:1616–1627. CrossRef Medline

Yue Y, Zhang D, Jiang S, Li A, Guo A, Wu X, Xia X, Cheng H, Tao T, Gu X (2014) LIN28 expression in rat spinal cord after injury. Neurochem Res 39:862–874. CrossRef Medline

Zackenfels K, Oppenheim RW, Rohrer H (1995) Evidence for an important role of IGF-I and IGF-II for the early development of chick sympathetic neurons. Neuron 14:731–741. CrossRef Medline

Zhao C, Sun G, Li S, Lang MF, Yang S, Li W, Shi Y (2010) MicroRNA let-7b regulates neural stem cell proliferation and differentiation by targeting nuclear receptor TLX signaling. Proc Natl Acad Sci U S A 107:1876–1881. CrossRef Medline

Zhou J, Ng SB, Chng WJ (2013) LIN28/LIN28B: an emerging oncogenic driver in cancer stem cells. Int J Biochem Cell Biol 45:973–978. CrossRef Medline